International Journal for Innovative Engineering and Management Research
A Peer Revieved Open Access International Journal
www.ijiemr.org

COPY RIGHT

2017 IJIEMR.Personal use of this material is permitted. Permission from IJIEMR must be obtained for all other uses, in any current or future media, including reprinting/republishing this material for advertising or promotional purposes, creating new collective works, for resale or redistribution to servers or lists, or reuse of any copyrighted component of this work in other works. No Reprint should be done to this paper, all copy right is authenticated to Paper Authors

IJIEMR Transactions, online available on 28th Aug 2017. Link :http://www.ijiemr.org/downloads.php?vol=Volume-6&issue=ISSUE-7

Title: **NON-ISOLATED BI-DIRECTIONAL SOFT-SWITCHING DC-DC CONVERTER FOR INDUSTRIAL APPLICATIONS**

Volume 06, Issue 07, Pages: 369-379.

Paper Authors

PADALA DANIEL ASHADEEP, KENGUVA ASHOK KUMAR
Pydah College of Engineering & Technology, Visakhapatnam,AP.

USE THIS BARCODE TO ACCESS YOUR ONLINE PAPER

To Secure Your Paper As Per UGC Guidelines We Are Providing A Electronic Bar Code

International Journal for Innovative Engineering and Management Research
A Peer Revieved Open Access International Journal
www.ijiemr.org

NON-ISOLATED BI-DIRECTIONAL SOFT-SWITCHING DC-DC CONVERTER FOR INDUSTRIAL APPLICATIONS

[1]PADALA DANIEL ASHADEEP, [2]KENGUVA ASHOK KUMAR

[1]M-Tech Student Scholar,Department of E.E.E,Pydah College of Engineering & Technology, Visakhapatnam,AP.
[2]Assistant ProfessorDepartment of E.E.E,Pydah College of Engineering & Technology, Visakhapatnam A.P.

Abstract: This paper proposes a new isolated, three-port, bidirectional soft switching DC-DC converter for integrating Ac and Dc micro grid. The proposed converter has the advantage of using the least number of switches and soft switching for the main switch, which is realized by using a LCL-resonant circuit. The converter is capable of interfacing sources of different voltage-current characteristics with a load and/or a DC micro grid. To improve performance the micro grids in integrated with main grid or standalone operations by using an efficient controllers and with high efficient converters/inverters. Non-isolated converters have obvious merits of lower magnetic bulk, higher efficiency, and compactness. To improve power density high-frequency operation of dc/dc converter is necessary. However, at high device switching frequency, switching transition losses in semiconductor devices are very high; therefore, and soft-switching is desired. For the aforesaid reasons, micro grids are gaining popularity for power generation and distribution. Solar photovoltaic, fuel cells, and battery output are available for use in dc form. Therefore, another stage of conversion is required before its interconnection with ac system or regulated dc system. Dc grid is an alternative. Because the renewable energy sources are highly intermittent, energy storage is required to supply continuous power to the load. Micro grids are the possibility to generate electric power with lower environmental impact and easier connection of these sources to the utility, including the power management capability among their elements. In extension we are integrating the converter to an induction motor drive is presented by using MATLAB/SIMULINK Software.

Key Words: . microgrid, soft switching, dc-dc converter, induction motor drive.

I. INTRODUTION

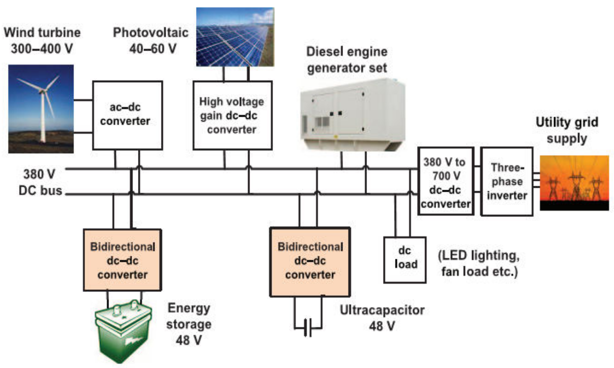

Fig.1. Typical configuration of dc microgrid.

This paper proposes a soft-switching non-isolated bidirectional LCL resonant dc/dc converter as shown in Fig.2. It has front-end half-bridge boost converter followed by an LCL resonant tank, and voltage doubler at high voltage side. The proposed converter has the following merits: 1) zero-voltage switching (ZVS) turn-on of all switches in both directions; 2) zero-current-switching (ZCS) turn-on and turn-off of all diodes in both directions; 3) low

International Journal for Innovative Engineering and Management Research
A Peer Revieved Open Access International Journal
www.ijiemr.org

voltage stress across semiconductor devices; 4) device voltage is clamped without additional snubber circuit; 5) high step up and step down ratio; and 6) reduced volume of magnetics.

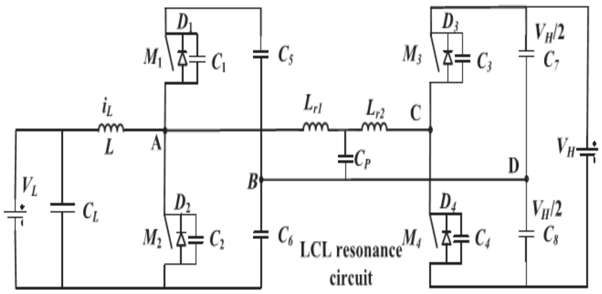

Fig.2. Proposed bidirectional LCL resonant dc/dc converter.

II. OPERATION AND ANALYSIS OF THE CONVERTER

Fig.2 shows the proposed bidirectional dc/dc converter. LCL resonant circuit increases the voltage gain and provides ZVS of front-end devices and ZCS of diodes. For boost operation, front-end half-bridge current-fed converter offers a voltage gain of and LCL resonant circuit adds an additional gain depending on the ratio of resonant to switching frequency. Voltage doubler at output offers additional gain of 2×. In buck operation, the high voltage is divided by capacitor divider to half. Further, switches M_3 and M_4 are modulated to allow high step down ratio. The LCL resonant circuit aids in ZVS of switches M_3 and M_4 and ZCS of diodes D_1 and D_2.Gating signals of M_1 and M_2 are complementary with each other with enough dead band for boost operation. M_3 and M_4 are in OFF-state. M_3 and M_4 are operated complementary with each other with enough dead time for buck operation. M_1 and M_2 are not modulated. The steady-state operation of converter in both buck and boost operating modes is explained next.

A. Boost Operation

The steady-state operating waveforms and the equivalent circuits of operation in boost mode are shown in Figs.3 and 4, respectively. Devices M_3 and M_4 are not triggered and remain in OFF-state for entire boost operation.

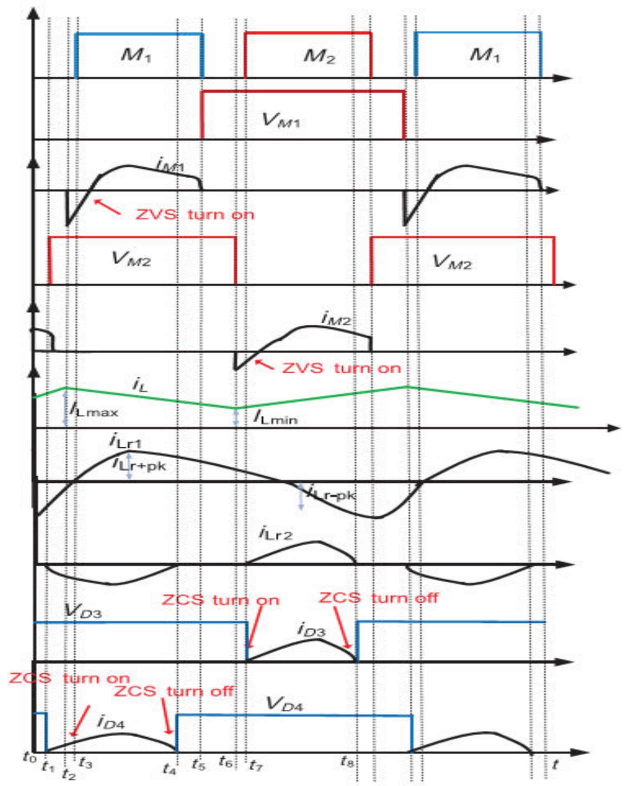

Fig.3. Theoretical waveform for boost operation.

Interval 1 [Fig.4 (a): $t_0 < t < t_1$]: The converter is operating like a boost converter. Switch M_2 is conducting and inductor L is storing energy. Switch M_1 and high side body-diodes are in OFF-state. Power is transferred to load by output capacitors C_7 and C_8.

Interval 2 [Fig.4 (b): $t_1 < t < t_2$]: At $t = t_2$, switch M_2 is turned-off. Now both the switches M_1 and M_2 are OFF. Input inductor current i_L and resonant current i_{Lr1} jointly start discharging and charging the device parasitic capacitances C_1 and C_2, respectively. At end of this interval,

International Journal for Innovative Engineering and Management Research
A Peer Revieved Open Access International Journal
www.ijiemr.org

C_1 is discharged and C_2 is charged completely. This is quick and the duration is very short.

Final values are i_{M1} (t_2) = 0, i_{M2} (t_2) = 0, v_{M1} (t_2) = 0, and v_{D4} (t_2) = 0. Voltage across switch M_2 is given by

$$v_{M2}(t_1) = \frac{V_L}{1-D}. \quad (1)$$

Duty ratio of the switches, $D = T_{ON}/T_s$; T_{ON} = conduction time of main switch; and T_s = switching period. Voltage across diode D_3 is given by

$$v_{D3} = V_H. \quad (2)$$

Interval 3 [Fig.4 (c): $t_2 < t < t_3$]: Now, the body diode D_1 starts conducting by the difference of input inductor current i_L and resonant inductor current i_{Lr1} causing zero voltage across M_1. Diode D_4 is forward biased and current starts flowing through resonant inductor L_{r2} and capacitor C_P starts charging output capacitor C_8. Final values are i_{M1} (t_3) = 0, i_{M2} (t_3) = 0, v_{M1} (t_3) = 0, v_{M2} (t_3) = $V_L/1-D$

$$i_{D1}(t_3) = i_L(t_3) - i_{Lr1}(t_3) \quad (3)$$

Interval 4 [Fig.4 (d): $t_3 < t < t_4$]: At $t = t_3$, M_1 starts conducting with ZVS. The equivalent resonant circuit is shown in Fig.5 (a). Antiparallel body-diode D_4 is still conducting to charge capacitor C_8 while antiparallel diode D_3 is reverse biased. At the end of this interval, diode D_4 turns off with ZCS as the resonant inductor current i_{Lr2} discontinues to zero. The equations for this interval are

$$i_{Lr1}(t) = \frac{v_{C_5}(t_3) - v_{C_P}(t_3)}{Z_r} \cdot \sin w_r(t - t_3) \quad (4)$$

Where

$$w_r = \sqrt{\frac{C_5 + C_P}{L_{r1}C_P C_5}} \text{ and } z_r = \sqrt{\frac{L_{r1}(C_5 + C_P)}{C_5 C_P}}$$

$$i_L(t) = i_L(t_3) - \frac{V_L - v_{C_5}(t_2) - v_{C_6}(t_2)}{L}(t - t_3) \quad (5)$$

$$i_{M1}(t) = i_{Lr1}(t) - i_L(t). \quad (6)$$

Voltage across antiparallel diode D_3 is

$$v_{D3} = V_H \quad (7)$$

Where Z_r is known as characteristic impedance offered by the circuit formed by resonant tank L_{r1}, C_p, and capacitor C_5 as shown in Fig.5 (a).

Interval 5 [Fig.4 (e): $t_4 < t < t_5$]: Switch M_1continues to conduct and output antiparallel body-diodes are reverse-biased.

The power to the load is supplied by energy stored in output capacitor C_7 and C_8.At $t = t_4$, switch M_1 is turned-off. Final values are v_{D3} (t_5) = 0, v_{D4} (t_5) = 0, v_{M2} (t_5) = $V_L/1-D$.

Interval 6 [Fig.4 (f): $t_5 < t < t_6$]: Parasitic capacitance C_1 is charged and parasitic capacitance C_2 is discharged by difference of resonant inductor current i_{Lr1} and boost inductor current i_L. High side body-diodes are reverse biased. At end of this interval, capacitance C_2 is discharged completely and C_1 is charged to $V_H/1-D$.

Interval 7 [Fig.4 (g): $t_6 < t < t_7$]: In this interval, antiparallel body-diode D_2 starts conducting through a difference of ($i_{Lr} - i_L$) and M_2 can now be gated for ZVS turn-on. At output, antiparallel body-diode D_4 is reverse-biased while D_3 conducts. Final values are i_{M1} (t_7) = 0, i_{M2} (t_7) = 0, v_{M1} (t_7) = 0, v_{M2} (t_7) = $V_{in}/1-D$

$$i_{D2}(t_7) = i_L(t_7) - i_{Lr1}(t_7) \quad (8)$$

Interval 8 [Fig.4 (h): $t_7 < t < t_8$]: At $t = t_7$, switch M_2 conducts with ZVS. Resonant inductor L_r, capacitor C_P, and C_4 resonate together as shown in Fig.5 (b). At end of this interval $t = t_8$, body-diode D_3 turns off with ZCS. The resonant current through L_r is given by

International Journal for Innovative Engineering and Management Research
A Peer Revieved Open Access International Journal
www.ijiemr.org

$$i_{Lr1} = -\frac{v_{C_6}(t_7) + v_{C_P}(t_7)}{Z_r} \sin w_r \ (t - t_7) \tag{9}$$

Where

and for $C_5 = C_6$

Here, characteristic impedance Z_r is offered by the circuit formed by L_{r1}, C_p, and capacitor C_6 as shown in Fig.5 (b). Current through boost inductor L is given by

$$i_L(t) = i_L(t_7) + \frac{V_L}{L}(t - t_7) \tag{10}$$

Current through switch M_2 is given by

$$i_{M2} = i_L(t - t_7) - i_{Lr1}(t - t_7) \tag{11}$$

Then, next half cycle starts with the symmetrical devices conducting to complete the full HF cycle.

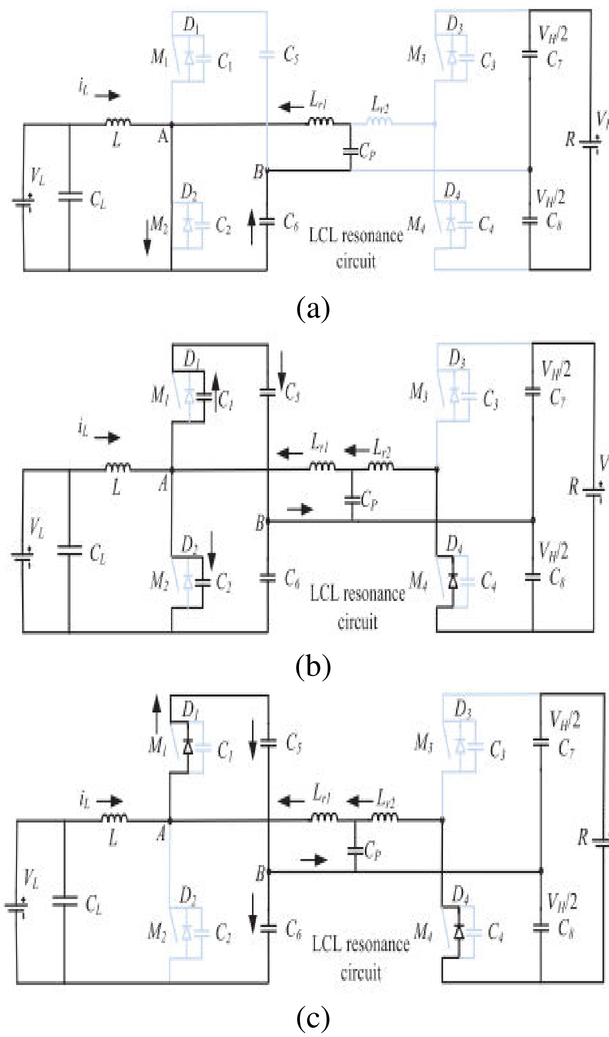

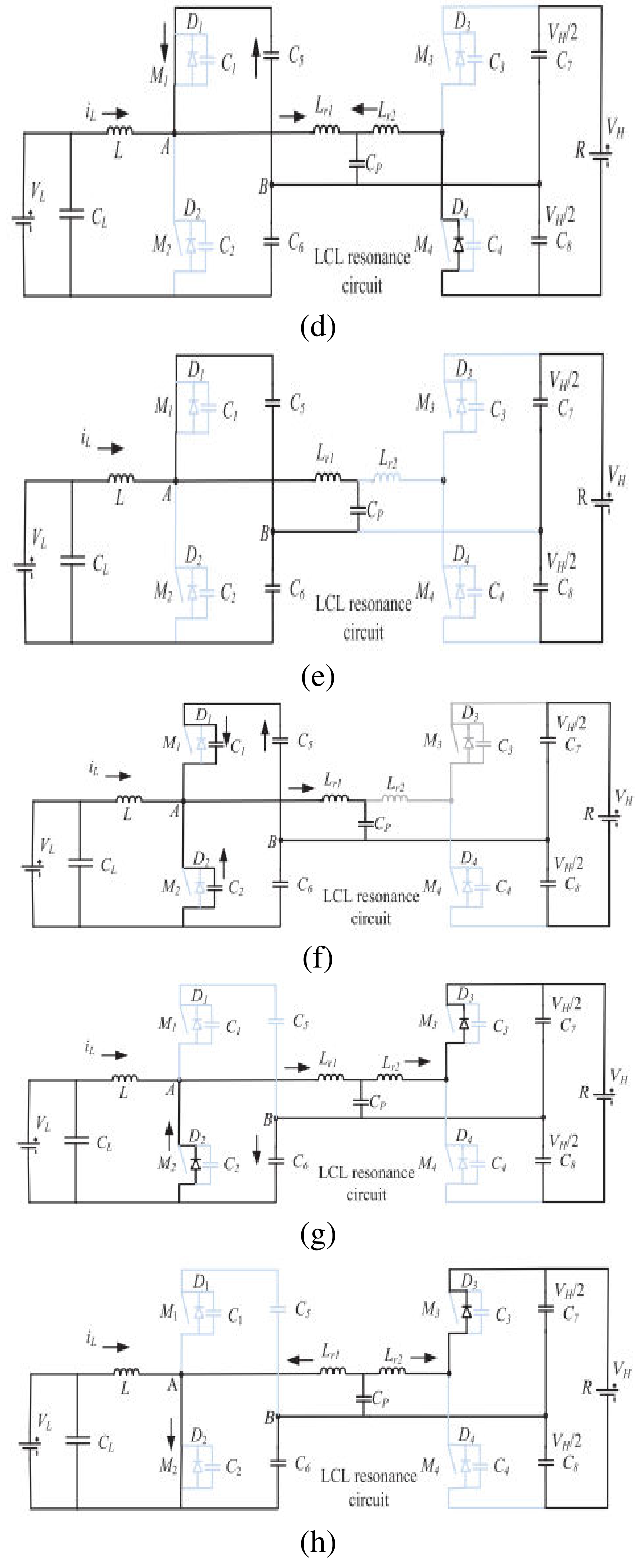

Fig.4. Equivalent circuits during different intervals of operation of the proposed converter in boost operation.

International Journal for Innovative Engineering and Management Research
A Peer Revieved Open Access International Journal
www.ijiemr.org

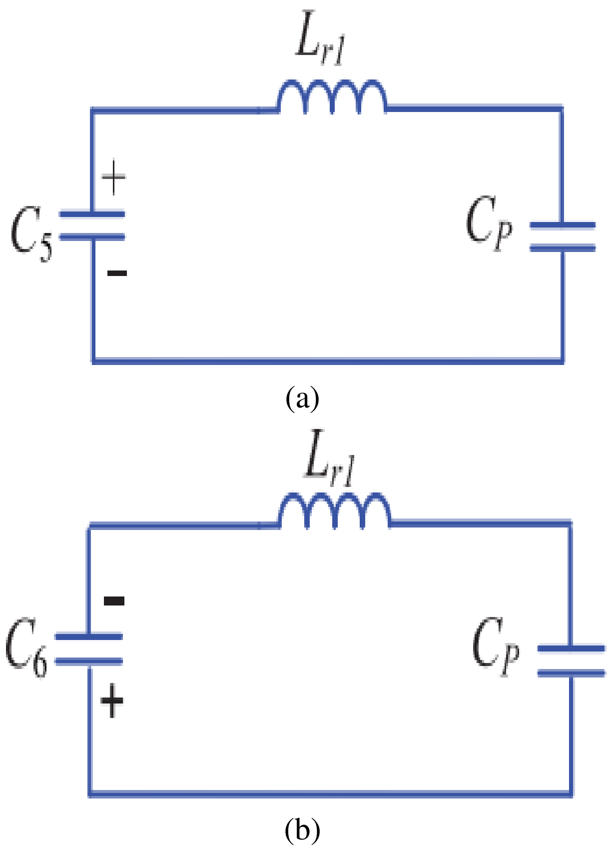

Fig.5. Equivalent circuit for resonant operation in (a) Interval 3 and (b) Interval 7.

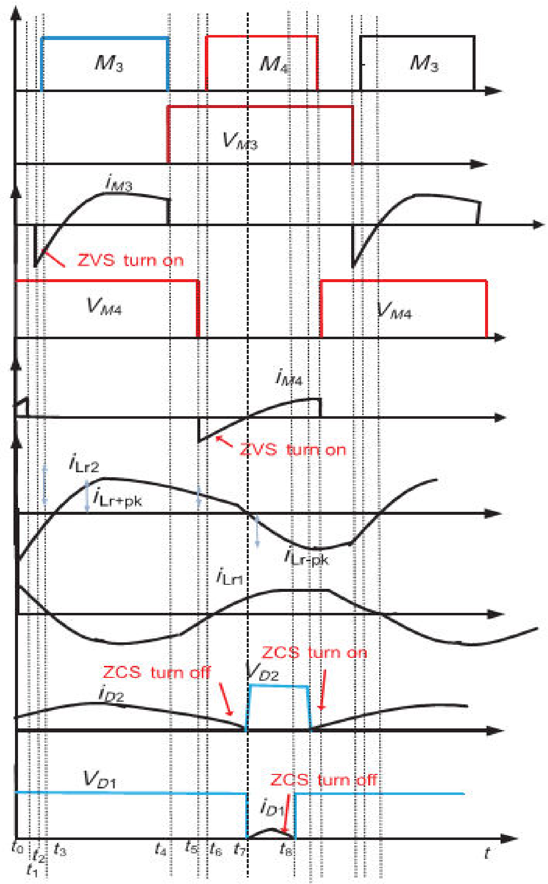

Fig.6. Theoretical waveforms in buck operation.

3.2.2 Buck Operation

The steady-state operating waveforms and the equivalent circuits representing the different intervals of operation for the buck mode are shown in Figs.6 and 7, respectively. M_1 and M_2 are not triggered for entire buck operation.

Interval 1 [Fig.7 (a): $t_0 < t < t_1$]: It is identical to buck or voltage-fed operation. Switch M_4 is conducting and power is transferred to low voltage side through resonant circuit and body diode D_2. Resonant current flows in the circuit.

Interval 2 [Fig.7 (b): $t_1 < t < t_2$]: At $t = t_1$, switch M_4 is turned-off. Parasitic capacitances C_3 and C_4 start charging and discharging, respectively, by resonant current i_{Lr2}. At end of this interval, C_3 and C_4 are fully discharged and charged (to V_H), respectively. This is a quick and short interval. Resonant inductor current i_{Lr1} is given by

$$i_{Lr1}(t) = \frac{v_{C_P}(t_1) + v_{C_6}(t_1)}{Z_r} \cdot \sin w_r (t - t_1) \tag{12}$$

Where

and for $C_5 = C_6$

Current through inductor L is given by

International Journal for Innovative Engineering and Management Research
A Peer Revieved Open Access International Journal
www.ijiemr.org

$$i_L(t) = i_L(t_1) - \frac{V_L}{L}(t - t_1) \tag{13}$$

Current through diode D_2 is given by

$$i_{D2}(t - t_1) = i_{\mathrm{Lr1}}(t - t_1) - i_L(t - t_1) \tag{14}$$

Final values are $i_{M3}(t_2) = 0$, $i_{M4}(t_2) = 0$, $v_{M3}(t_2) = V_H$, and $v_{M4}(t_2) = 0$.

Interval 3 [Fig.7 (c): $t_2 < t < t_3$]: The resonant inductor current i_{Lr2} flows through antiparallel body diode D_3 causing zero voltage across switch M_3 and it can be gated for ZVS turn-on. Current through resonant inductor L_{r2} is given by

$$i_{\mathrm{Lr2}}(t) = \frac{v_{C_P}(t_2) + 0.5V_H}{Z_{\mathrm{rb}}} \cdot \sin w_{\mathrm{rb}}(t - t_2) \tag{15}$$

Where

Current through antiparallel diode D_3 is given by

$$i_{D3}(t) = i_{\mathrm{Lr2}}(t). \tag{16}$$

Final values are $i_{M3}(t_3) = 0$, $i_{M4}(t_3) = 0$, $v_{M3}(t_3) = 0$, and $v_{M4}(t_3) = V_H$.

Interval 4 [Fig.7 (d): $t_3 < t < t_4$]: At $t = t_3$, switch M_3 turns on with ZVS. Voltage $V_H/2$ is applied across resonant circuit through switch M_3. Resonant inductor L_{r2} and capacitor C_P resonate with capacitor C_7. This interval end at $t = t_4$ when switch M_3 is turned-off.

Interval 5 [Fig.7 (e): $t_4 < t < t_5$]: In this interval, both the switches M_3 and M_4 are off. Parasitic capacitances C_4 and C_3 start discharging and charging, respectively, by resonant current i_{Lr2}. At $t = t_5$, C_4 is discharged completely and C_3 is fully charged to V_H. Final values are $i_{M3}(t_5) = i_{M4}(t_5) = 0$, $v_{M3}(t_5) = V_H$, and $v_{M4}(t_5) = 0$.

Interval 6 [Fig.7 (f): $t_5 < t < t_6$]: Antiparallel diode D_4 start conducting and M_4 can now be gated for ZVS turn-on. At end of this interval antiparallel diode D_2 turns off with ZCS. Current through resonant inductor L_{r2} is given by

$$i_{\mathrm{Lr2}}(t) = \frac{v_{C_P}(t_5) + 0.5V_H}{Z_{\mathrm{rb}}} \cdot \sin w_{\mathrm{rb}}(t - t_5) \tag{17}$$

Where

and

Current through antiparallel diode D_3 is given by

$$i_{D4} = i_{\mathrm{Lr2}}. \tag{18}$$

Final values are $i_{M3}(t_6) = i_{M4}(t_6) = 0$, $v_{M4}(t_6) = 0$, and $v_{M3}(t_6) = V_H$.

Interval 7 [Fig.7 (g): $t_6 < t < t_7$]: At $t = t_6$, switch M_4 turns on with ZVS. Therefore, resonant current i_{Lr2} is diverted through switch M_4. Antiparallel diode D_1 is forward biased and starts charging capacitor C_5. At $t = t_7$, antiparallel diode D_1 turns off with ZCS.

Then, next half cycle starts with the symmetrical devices conducting to complete the full HF cycle.

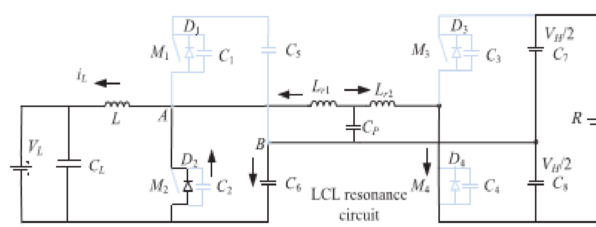

(a)

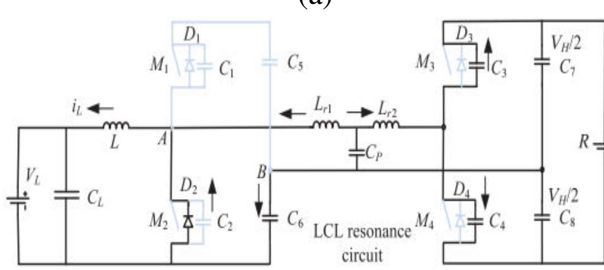

(b)

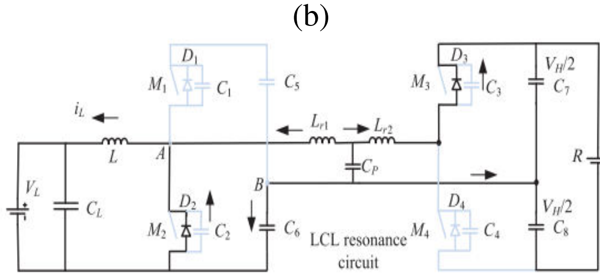

(c)

International Journal for Innovative Engineering and Management Research
A Peer Revieved Open Access International Journal
www.ijiemr.org

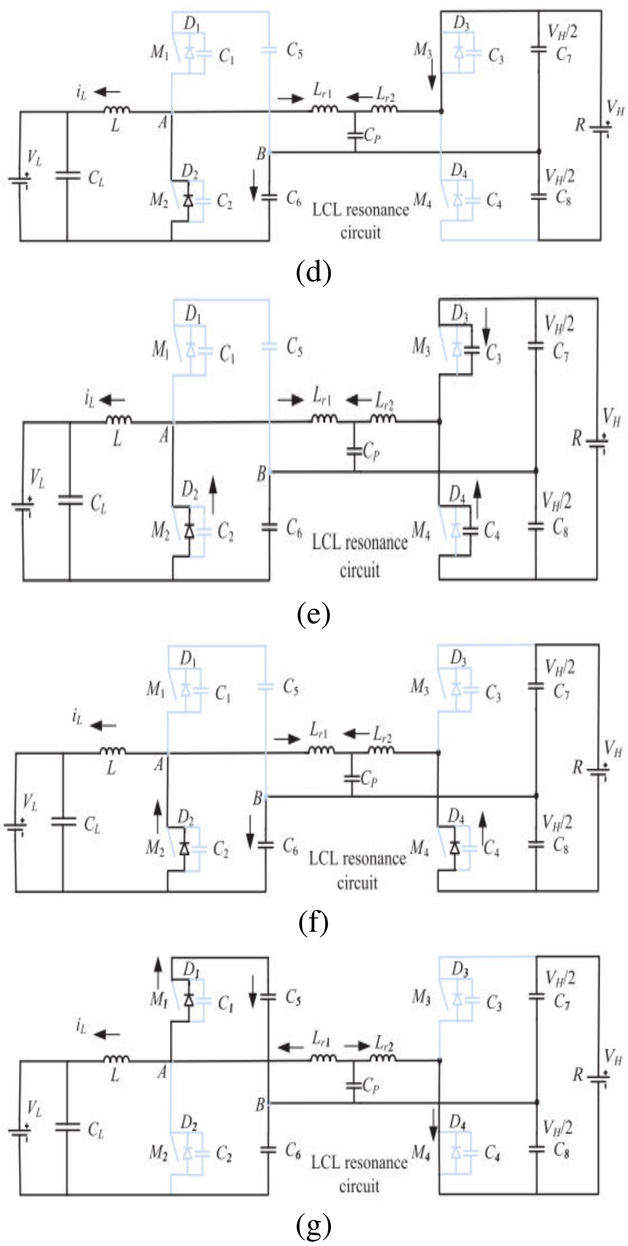

Fig.7. Equivalent circuits during different intervals of buck operation.

III. VOLTAGE GAIN AND SOFT-SWITCHING CONDITIONS

A. Voltage Gain

1) Boost Mode: The converter has three stages that contribute to its overall voltage gain. 1) Front-end boost converter gain = $V_{in}/ (1-D)$; 2) resonant circuit gain; and 3) voltage doubler gain = 2×. The overall converter gain is the multiplication of the gains offered by the individual circuits and is given by

$$V_H = \frac{V_L \cdot G_{\text{boost}} \cdot 2}{1-D} \tag{19}$$

Where

D is duty cycle, fs is the switching frequency, R_{ac} is effective ac load resistance and is given by R_{ac} = , X_{cp}, X_{Lr1}, X_{Lr2}, X_{C6} are reactance of C_p, L_{r1}, L_{r2}, C_6, respectively. It is straightforward to derive using standard complex ac analysis.

2) Buck Mode: In the buck mode, $V_H/2$ is applied across the resonant circuit due to capacitor voltage divider circuit. The overall step down ratio is given by

$$V_L = 0.5V_H \cdot D_{\text{buck}} G_{\text{buck}} \tag{20}$$

Where

B. ZVS Conditions

To ensure ZVS of upper switch M_1, energy stored in resonant inductor L_{r1} at $t = t_1$ has to be greater than energy stored in device capacitance of switch M_1 and M_2 and is given by

$$\frac{1}{2} L_{r1} I^2_{\text{Lavg}} - \frac{1}{2} L_{r1} i^2_{r1}(t1) > \frac{1}{2}(C_1 + C_2)\left(\frac{V_{\text{in}}}{1-D}\right)^2 \tag{21}$$

To achieve ZVS of bottom switch M_2, the difference between energy stored in the resonant inductor L_{r1} and input inductor L must be sufficient to charge device capacitance C_1 and discharge C_2 and it is given by

$$\frac{1}{2} L_{r1} I^2_{\text{Lavg}} - \frac{1}{2} L_{r1} i^2_{r1}(t5) > \frac{1}{2}(C_1 + C_2)\left(\frac{V_{\text{in}}}{1-D}\right)^2 \tag{22}$$

INDUCTION MOTOR (IM)

An induction motor is an example of asynchronous AC machine, which consists of a stator and a rotor. This motor is widely used because of its strong features and reasonable

International Journal for Innovative Engineering and Management Research
A Peer Revieved Open Access International Journal
www.ijiemr.org

cost. A sinusoidal voltage is applied to the stator, in the induction motor, which results in an induced electromagnetic field. A current in the rotor is induced due to this field, which creates another field that tries to align with the stator field, causing the rotor to spin. A slip is created between these fields, when a load is applied to the motor. Compared to the synchronous speed, the rotor speed decreases, at higher slip values. The frequency of the stator voltage controls the synchronous speed. The frequency of the voltage is applied to the stator through power electronic devices, which allows the control of the speed of the motor. The research is using techniques, which implement a constant voltage to frequency ratio. Finally, the torque begins to fall when the motor reaches the synchronous speed. Thus, induction motor synchronous speed is defined by following equation,

$$n_s = \frac{120f}{P}$$

Where f is the frequency of AC supply, n, is the speed of rotor; p is the number of poles per phase of the motor. By varying the frequency of control circuit through AC supply, the rotor speed will change.

A. Control Strategy of Induction Motor

Power electronics interface such as three-phase SPWM inverter using constant closed loop Volts l Hertz control scheme is used to control the motor. According to the desired output speed, the amplitude and frequency of the reference (sinusoidal) signals will change. In order to maintain constant magnetic flux in the motor, the ratio of the voltage amplitude to voltage frequency will be kept constant. Hence a closed loop Proportional Integral (PI) controller is implemented to regulate the motor speed to the desired set point. The closed loop speed control is characterized by the measurement of the actual motor speed, which is compared to the reference speed while the error signal is generated. The magnitude and polarity of the error signal correspond to the difference between the actual and required speed. The PI controller generates the corrected motor stator frequency to compensate for the error, based on the speed error.

IV. MATLAB /SIMULINK RESULTS

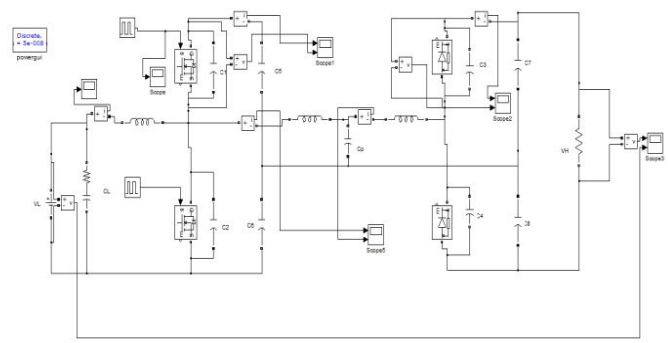

Fig.8 shows the matlab/Simulink model of proposed dc-dc converter in boost mode

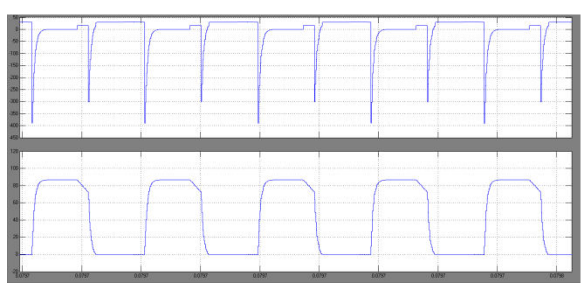

Fig.9 shows the voltage and current of switch

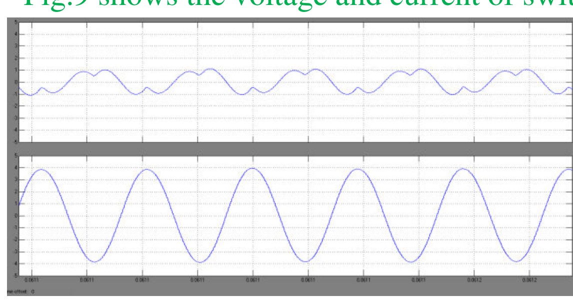

Fig.10 shows the currents of resonant inductors

International Journal for Innovative Engineering and Management Research
A Peer Revieved Open Access International Journal
www.ijiemr.org

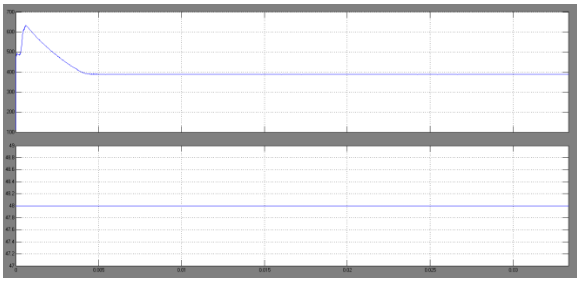

Fig.11 shows the output voltage and input voltage of boost mode

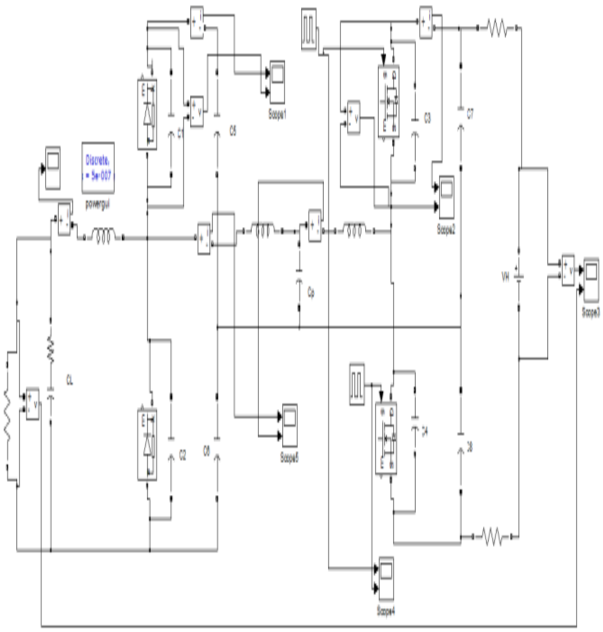

Fig.12 shows the matlab/Simulink model of proposed dc-dc converter in buck mode

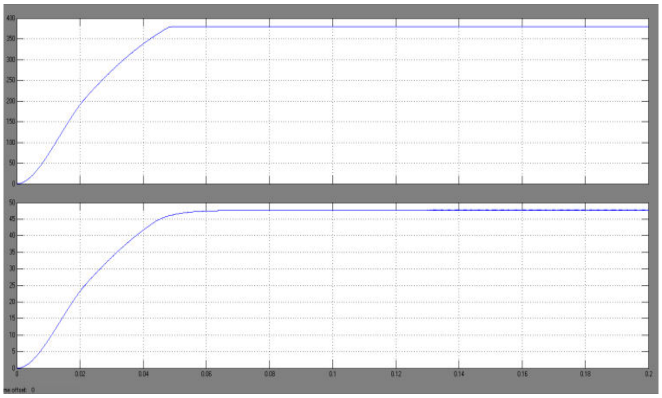

Fig.13 shows the output voltage and input voltage of boost mode

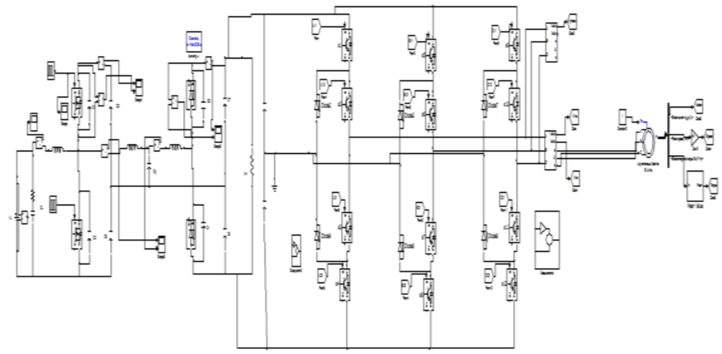

Fig.14 shows the matlab/Simulink model of proposed dc-dc converter in boost mode with induction motor drive

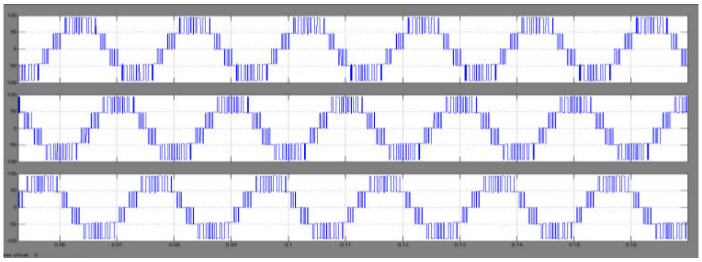

Fig.15 shows the line voltage of inverter operating as five level inverter

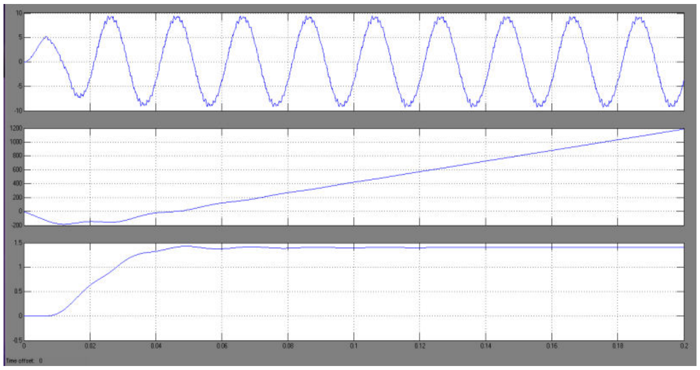

Fig.16 shows the performance of induction motor drive

V. CONCLUSION

A non-isolated bidirectional soft-switchingcurrent-fed resonant dc/dc converter was proposed. The key features are high step up/step down ratio, high efficiency, low device voltage stress, and soft-switching, i.e., ZVS turn-on for all switches and ZCS turn-on and

International Journal for Innovative Engineering and Management Research
A Peer Revieved Open Access International Journal
www.ijiemr.org

turn-off for all diodes in both buck/boost mode of operation. Proposed converter achieves ZVS for switches and ZCS for diodes over a wide load range. Device voltage is also clamped without any snubber circuit. The proposed system is connected to an induction motor drive and performance of the drive is observed.

REFERENCES

[1] R. H. Lasseter and P. Paigi, “Microgrid: A conceptual solution,” in Proc. IEEE Power Electron. Spec. Conf. (PESC’04), Jun. 2004, vol. 6, pp. 4285–4290.

[2] Y. Ito, Y. Zhongqing, and H. Akagi, “DC microgrid based distribution power generation system,” in Proc. IEEE Power Electron. Motion Control Conf. (IPEMC’04), Aug. 2004, vol. 3, pp. 1740–1745.

[3] M. Gerber, J. A. Ferreira, N. Seliger, and I. W. Hofsajer, “Design and evaluation of an automotive integrated system module,” in Proc. IEEE Ind. Appl. Conf., Oct. 2005, vol. 2, pp. 1144–1151.

[4] H.-L. Do, “Non-isolated bidirectional zero-voltage-switching DC–DC converter,” IEEE Trans. Power Electron., vol. 26, no. 9, pp. 2563–2569, Sep. 2011.

[5] D. Zhang, D. Y. Chen, and F. C. Lee, “An experimental comparison of conducted EMI emissions between a zero-voltage transition circuit and a hard switching circuit,” in Proc. IEEE Power Electron. Spec. Conf. (PESC’04), 1996, pp. 1992–1997.

[6] W. Li, X. Lv, Y. Deng, J. Liu, and X. He, “A review of non-isolated high step-up DC/DC converters in renewable energy applications,” in Proc. 24th Annu. IEEE Appl. Power Electron. Conf. Expo., 2009, pp. 364–369.

[7] X. Li and A. K. S. Bhat “Analysis and design of high-frequency isolated dual-bridge series resonant DC/DC converter,” IEEE Trans. Power Electron., vol. 25, no. 4, pp. 850–862, Apr. 2010.

[8] S. Han and D. Divan, “Bi-directional DC/DC converters for plug-in hybrid electric vehicle (PHEV) applications,” inProc. 23rd Annu. IEEE Appl. Power Electron. Conf. Expo. (APEC’08), 2008, pp. 784–789.

[9] P. Xuewei and A. K. Rathore, “Novel bidirectional snubberless naturally commutated soft-switching current-fed full bridge isolated DC/DC converter for fuel cell vehicles,” IEEE Trans. Ind. Electron., vol. 61, no. 5, pp. 2307–2315, May 2014.

[10] R. J. Wai and R. Y. Duan, “High-efficiency bidirectional converter for power sources with great voltage diversity,” IEEE Trans. Power Electron., vol. 22, no. 5, pp. 1986–1996, Sep. 2007.

[11] U. R. Prasanna and A. K. Rathore, “Extended range ZVS active-clamped current-fed full-bridge isolated DC/DC converter for fuel cell applications: Analysis, design and experimental results,” IEEE Trans. Ind. Electron., vol. 60, no. 7, pp. 2661–2672, Jul. 2013.

[12] L. Jiang, C. C. Mi, S. Li, M. Zhang, X. Zhang, and C. Yin, “A novel soft switching bidirectional DC–DC converter with coupled inductors,” IEEE Trans. Ind. Appl., vol. 49, no. 6, pp. 2730–2740, Nov./Dec. 2013.

[13] M. Kwon, S. Oh, and S. Choi, “High gain soft-switching bidirectional DC–DC converter for eco-friendly vehicles,” IEEE Trans. Power Electron., vol. 29, no. 4, pp. 1659–1666, Apr. 2014.

[14] L. S. Yang and T. J. Liang, “Analysis and implementation of a novel bidirectional DC–DC

International Journal for Innovative Engineering and Management Research
A Peer Revieved Open Access International Journal
www.ijiemr.org

converter," IEEE Trans. Ind. Electron., vol. 59, no. 1, pp. 422–434, Jan. 2012.

[15] Y.-P. Hsieh et al., "High-conversion-ratio bidirectional DC–DC converter with coupled inductor," IEEE Trans. Ind. Electron., vol. 61, no. 1, pp. 210–222, Jan. 2014.

[16] R. J. Wai, R. Y. Duan, and K. H. Jheng, "High-efficiency bidirectional DC–DC converter with high-voltage gain," IET Power Electron., vol.5, no. 2, pp. 173–184, 2012.

[17] T. Liang and H. Liang, "Analysis, design and implementation of a bidirectional double-boost DC–DC converter," IEEE Trans. Ind. Appl., vol. 59, no. 1, pp. 422–434, Jan./Feb. 2012.

[18] L. A. Flores, O. Garcia, J. A. Oliver, and J. A. Cobos, "High-frequency bidirectional DC/DC converter using two inductor rectifier," in Proc. IEEE Int. Power Electron. Congr., 2006, pp. 2793–2798.

[19] Y.-S. Lee and Y.-Y. Chiu, "Zero current switching switched-capacitor bidirectional DC–DC converter," Proc. Inst. Elect. Eng., vol. 152, no. 6, pp. 1525–1530, 2005.

[20] H. S. H. Chung and W. C. Chow, "Development of a switched-capacitor DC/DC converter with bidirectional power flow," IEEE Trans. Circuits Syst. I, Fundam. Theory Appl., vol. 47, no. 9, pp. 1383–1389, Sep. 2000

Authors profile:

PADALA DANIEL ASHADEEP Received B.Tech Degree From Swarnandhra Institute Of Enginerring And Technology In The Year 2015 And Now Pursuing M.Tech In The Stream Of Electrical Power Systems At Pydah College Of Engineering.

KENGUVA ASHOK KUMAR Received B.Tech Degree From BVEC In The Year 2012 And Received M.Tech In The Stream Of Electrical Power Systems At BVCITS. Currently Working As Assistant Professor In PYDAH College Of Engineering And Technology Since 2.5 Years And Also The Member Of IJEEE. And His Areas of Interest Are Power Systems, Switch Gears.